

Nanoscale

Accepted Manuscript



This is an *Accepted Manuscript*, which has been through the Royal Society of Chemistry peer review process and has been accepted for publication.

Accepted Manuscripts are published online shortly after acceptance, before technical editing, formatting and proof reading. Using this free service, authors can make their results available to the community, in citable form, before we publish the edited article. We will replace this *Accepted Manuscript* with the edited and formatted *Advance Article* as soon as it is available.

You can find more information about *Accepted Manuscripts* in the [Information for Authors](#).

Please note that technical editing may introduce minor changes to the text and/or graphics, which may alter content. The journal's standard [Terms & Conditions](#) and the [Ethical guidelines](#) still apply. In no event shall the Royal Society of Chemistry be held responsible for any errors or omissions in this *Accepted Manuscript* or any consequences arising from the use of any information it contains.

PAPER

Graphene/polyaniline woven fabric composite films as flexible supercapacitor electrodes

Cite this: DOI: 10.1039/x0xx00000x

Xiaobei Zang,^a Xiao Li,^{a,b} Miao Zhu,^{a,b} Xinming Li,^c Zhen Zhen,^{a,b} Yijia He,^{a,b} Kunlin Wang,^a Jinquan Wei,^a Feiyu Kang^{a,d} and Hongwei Zhu^{a,b*}

Received 00th January 2014,

Accepted 00th January 2014

DOI: 10.1039/x0xx00000x

www.rsc.org/

We report the design and preparation of graphene and polyaniline (PANI) woven-fabric composite films by *in-situ* electropolymerization. The introduction of PANI greatly improves the electrochemical properties of solid-state supercapacitors which possess capacitances as high as 23 mF/cm², and exhibit excellent cycling stability with ~100% of capacitance retention after 2000 cycles. The devices have displayed superior flexibility with improved areal specific capacitances to 118% during deformation.

Introduction

With the development of portable electronic equipment, for instance, flexible electronics, rollable displays and flexible solar cells, the energy storage devices are required to fulfil the flexibility¹. Flexible supercapacitors, as one of flexible energy storage devices, could satisfy the requirement of flexibility and storing energy^{2,3}. Supercapacitor, also called as electrochemical capacitor, has characteristics of long-cycle life, high power density. Flexible supercapacitor could change the device's shape to meet demand while electrochemical properties hold constant. While taking deformation resistance into account, the second moment of area increases with the increase of thickness. The thinner the device, the smaller the deformation resistance, and it is easier to be deformed. Thin film electrode materials is two dimensional (2D), which reduces the deformation resistance from the vertical direction. On the one hand, it makes the entire device thin, flexible and easy to be folded, twisted and reshaped. On the other hand, the structure shorten the travel distance of electrolyte ions.

Graphene is a 2D monolayer of sp² carbon materials⁴⁻⁶. Owing to the unique electrical, mechanical and chemical properties and high specific surface, graphene has been applied to energy storage devices^{7,8}. According to the energy storage mechanism, supercapacitors are classified into three types: electrical double-layer capacitors, pseudocapacitors and hybrid capacitors with electrical double-layer capacitors and pseudocapacitors^{9,10}. Carbon materials

such as activated carbon^{11,12}, mesoporous carbon^{13,14}, carbon nanotubes^{15,16} and graphene have been applied to electrical double-layer capacitors¹⁷⁻¹⁹. They store energy by ion adsorption, without any faradic charge transfer. The process can result in fast charge/discharge process, high power density and excellent cycling stability. However, the limited surface area and pore size distribution cause relatively low energy density²⁰. As a supplement, pseudocapacitors could increase the energy density sacrificing cycle life, flexibility and poor mechanical strength. Recent research efforts have focused on combining electrical double-layer capacitor with pseudocapacitor^{21,22}. Polyaniline (PANI) is one kind of conducting polymers which can store charges not only in the electrical double layer but by faradic charge transfer. As a result, the introduction of polyaniline can increase the specific capacitance of carbon electrodes. Meanwhile polyaniline is an environmental-friendly conducting polymer, and it is easy to synthesize and simple acid-doping/base-dedoping chemistry²³.

Composites of graphene and polyaniline have been investigated in many previous studies. Most of them used binder in the fabrication process. The binder impaired the electrical conductivity and complicated the process²⁴. The common method was *in-situ* chemical oxidative polymerization, the aniline monomer was mixed in graphene oxide (GO) solution to obtain reduced graphene oxide (rGO)/PANI complexes^{25,26}. Solution mixing was a simple method, and in the fabrication process, the pre-prepared graphene materials and PANI were mixed under stirring or ultrasonication^{27,28}. However, there are still some problems in those methods, such as complex procedure, time consuming and instability. *In-situ* electropolymerization does not need an oxidant, and has the advantages of short reaction time, operational simplicity²⁹.

Here, we report a simple process to obtain the hybrid films consisting of graphene woven fabric (GWF) and PANI, and assemble them into supercapacitors. We use an *in-situ* electropolymerization method, coating PANI on GWF film. The structure of GWF retains the network configuration of the copper mesh substrate, which makes the

GWF display both good dimensional stability and electrical conductivity. The unique structural characteristics of GWF films afford additional internal surface between the electrode material and the electrolyte, which provide abundant active surface for the absorption and desorption of electrolyte ions, eventually improving the electrochemical performance of devices. Due to the superior mechanical properties, GWFs are easily to be transferred to flexible substrates, fabricating flexible supercapacitors. The introduction of PANI greatly improves the capacitance of GWF-based supercapacitors (from 2 to 23 mF/cm², nearly 12 times) without weakening the flexibility. The composite films were characterized by scanning electron microscopy (SEM), Raman spectroscopy, X-ray photoelectron spectroscopy (XPS) and electrochemical station. The deformation test indicates the potential of the GWF+PANI film to be electrode materials for flexible supercapacitors.

Results and Discussion

The GWF films were synthesized by direct chemical vapor deposition (CVD) on copper meshes, which could be effectively removed with aqueous FeCl₃/HCl solution, eventually affording GWF deposited on polymer substrates^{30,31}. The preparation of GWF+PANI supercapacitor is illustrated in **Figure 1a**. First, GWF deposited on PET with silver wires as working electrodes was immersed in 0.5 M aniline solution containing 1 M HCl. The electropolymerization process was conducted under 0.8 V. The electropolymerization time was range from 2 to 30 min. After washing thoroughly in deionized water, the single electrode was obtained. Two symmetrical electrodes with the poly(vinyl alcohol) (PVA)-H₃PO₄ polymer gel electrolyte³² were assembled into a solid-state supercapacitor. According to the analysis of SEM observations (**Figure 1b,c**), the morphology was different before and after the electropolymerization.

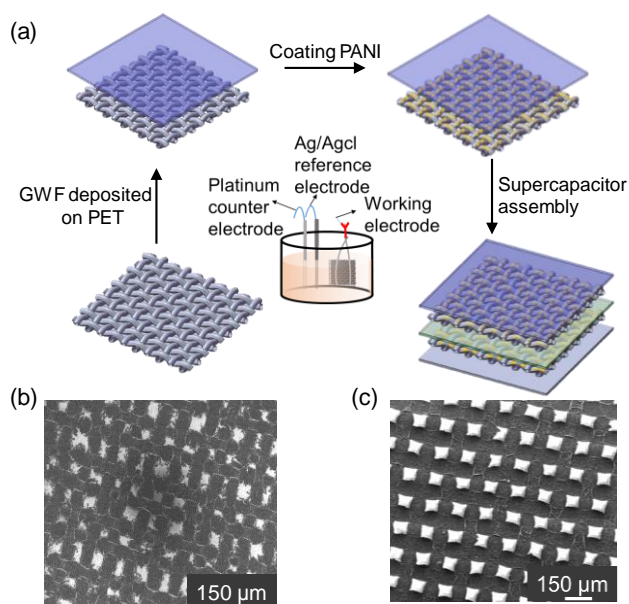


Fig. 1 (a) Illustration of preparation and fabrication process for GWF+PANI supercapacitor. SEM images of (b) GWF and (c) GWF+PANI films.

The woven fabric structure was clearly evident, and the mesh after electropolymerization was more bright and neat because charges concentrated in the cross section of GWF. The size of mesh was not modified evidently during this process. The electropolymerization time is a determining factor for electrochemical properties of the GWF+PANI based devices. As shown in **Figure 2a-c**, the coverage of PANI expanded with the time increasing from 2 to 15 min. At the same magnification, the PANI's configuration was strip-like but when the time reached 30 min, it changed to needle-like. The optimal electropolymerization time was 15 min. As seen in the high magnification images of GWF+PANI (15 min), the PANI owned granular aggregated structure (**Figure S1**). The Raman spectra of GWF and GWF+PANI are shown in **Figure 2e**, revealing the multilayer feature of graphene. The Raman spectrum of PANI showed characteristic peaks at 1162, 1338, 1507 and 1597cm⁻¹ indicating C-H bending of the quinoid ring, C-N⁺ stretching of the bipolaron form, N-H bending of the bipolaronic structure and C-C stretching of the benzenoid ring, respectively³³. Other disturbances caused by PET are shown in **Figure S2**.

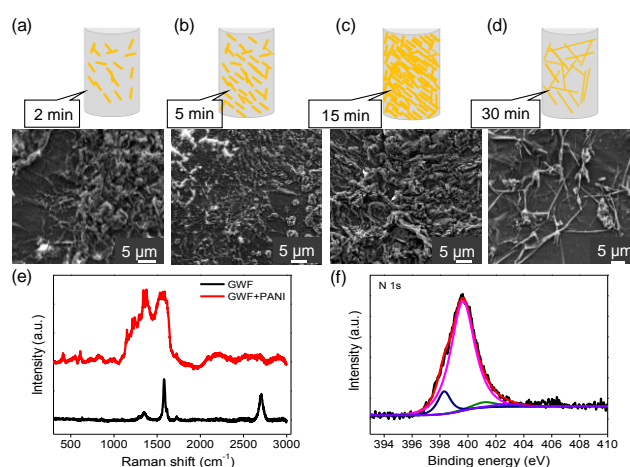


Fig. 2 Schematic illustrations and SEM images of GWFs coated with PANI at different electropolymerization times. (a) 2 min, (b) 5 min, (c) 15 min, and (d) 30 min. (e) Raman spectra of GWF and GWF+PANI (15 min). (f) XPS core-level spectrum of GWF+PANI (15 min).

To further understand the structural change of PANI in the doping/re-doping process, XPS analysis was conducted. As shown in **Figure 2f**, most of the nitrogen atoms was in three different forms: the benzenoid amine (-N-) centered at 399.7 eV, the quinoid amine (-N=) at 398.3 eV, and positively charged nitrogen atoms (N⁺) at 401.3 eV^{34,35}, indicating the successful redoping of PANI by HCl³⁶.

The electrochemical performance of supercapacitors was analyzed using the cyclic voltammogram (CV), galvanostatic charge-discharge test in a two-electrode system. **Figure 3a** compares the CV curves before and after electropolymerization on GWFs at a scan rate of 60 mV/s. Obviously, in the CV curve of GWF+PANI, the current density was higher than that of GWF, and the area of CV curve was also larger (the CV curve of GWF-based device is shown in **Figure S3a**). The results showed clearly the introduction of PANI could improve the electrochemical properties of GWF. The CV curves at lower scan rates (10 and 20 mV/s) show better rectangular shape, as shown in **Figure S3b**. The detailed CV curves of GWF+PANI at scan rates from 60 mV/s

to 1 V/s are shown in **Figure S4a**. CV curves deviated from the rectangular shape thanks to the pseudocapacitor behavior of the PANI. **Figure 3b** shows the galvanostatic charge-discharge curves of GWF and GWF+PANI. At a constant current (0.1 mA/cm^2), the charge/discharge time of GWF+PANI was longer than that of GWF. The areal specific capacitance could be obtained from the charge-discharge curve. It was originally 2 mF/cm^2 , while increased to 23 mF/cm^2 for the GWF+PANI composite electrode. As the current density increased to 2 mA/cm^2 (**Figure 3c**), the areal specific capacitance of GWF and GWF+PANI decreased to 0.7 and 6 mF/cm^2 respectively.

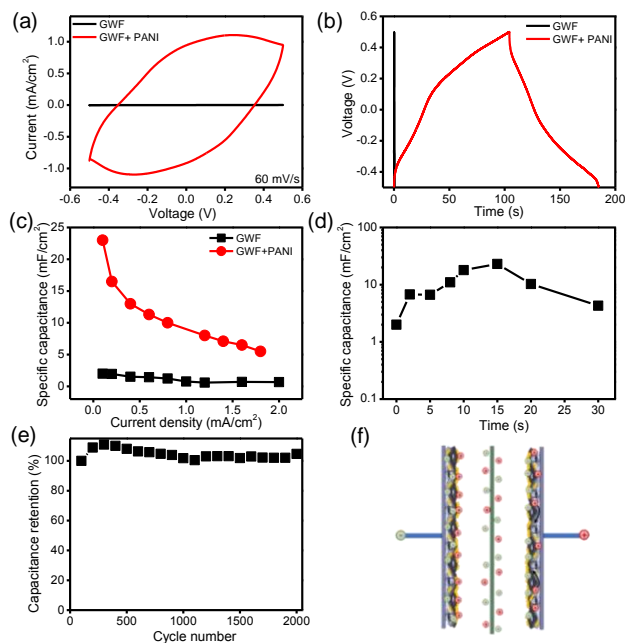


Fig. 3 Electrochemical performance of GWF+PANI (15 min) film supercapacitor. (a) CV curves (60 mV/s), (b) galvanostatic charge/discharge curves (0.1 mA/cm^2), (c) areal capacitances (0.1 to 2 mA/cm^2) of GWF and GWF+PANI. (d) Areal capacitance versus electropolymerization time. (e) Cycling stability and schematic illustration of the flexible GWF+PANI supercapacitor. (f) Schematic diagram of the GWF electrodes.

To investigate the effect of the electropolymerization time on the electrochemical performance of GWF+PANI electrode materials, we tested varied electropolymerization times of 2, 5, 8, 10, 15, 20 and 30 min. In the time range from 2 to 10 min, the areal capacitance increased from 7 to 18 mF/cm^2 (**Figure 3d**). For the time of 15 min, the areal capacitance raised up to 23 mF/cm^2 . However, as the time increased further to 20 min even 30 min, the areal capacitance dropped to 10 and 4 mF/cm^2 conversely, as a consequence of aggravating granular aggregation. It was confirmed by the CV curves and galvanostatic charge-discharge curves in **Figure S4b,c**. The optimal electropolymerization time was ~ 15 min.

From electrochemical impedance analysis from 0.01 Hz to 100 kHz , the electrochemical series resistance (ESR) could be obtained from the intercept of low frequency impedance spectrum with real axis. As shown in **Figure S4d**, the ESR of GWF+PANI (15 min) was 11Ω , lower than that of GWF (18Ω). In the low frequency range, GWF+PANI (15 min) presented the highest slope. Additionally, supercapacitors based

on GWF+PANI (15 min) possessed excellent stability, after 2000 cycles, it retained 100% areal specific capacitance of original capacity, as shown in **Figure 3e**. The role of GWF consists of three parts (**Figure 3f**): i) electrode materials to store charge; ii) current collector to transfer charge; iii) backbone for PANI electropolymerization. The mass loading of GWF film was 0.03 mg/cm^2 , and the mass specific capacitance of GWF device was 67 F/g at current density of 0.1 mA/cm^2 . The areal specific capacitance of GWF+PANI device increased nearly 12 times than that of GWF. In consequence, the mass specific capacitance of GWF+PANI device was $\sim 771 \text{ F/g}$, which was much higher than the values of other graphene/PANI supercapacitors (210 F/g of chemically converted graphene and polyaniline nanofibers composite films²⁸, 375.2 F/g of graphene nanosheets with polyaniline³⁵, and 763 F/g of graphene and polyaniline composite paper³⁸). In order to compare the overall performance of GWF and GWF+PANI, a Ragone plot is shown in **Figure S5**. The highest energy density of GWF+PANI device was 15 mWh/m^2 at power density of 0.33 mW/cm^2 . The highest power density was 1 mW/cm^2 at the energy density of 2.6 mWh/m^2 . While the highest energy density of GWF device was only 1.4 mWh/m^2 at power density of 0.03 mW/cm^2 . The highest power density was 0.3 mW/cm^2 at the energy density of 0.8 mWh/m^2 . A much higher energy density could be achieved by GWF+PANI than GWF and the values were higher than those reported in previous studies³⁹⁻⁴¹.

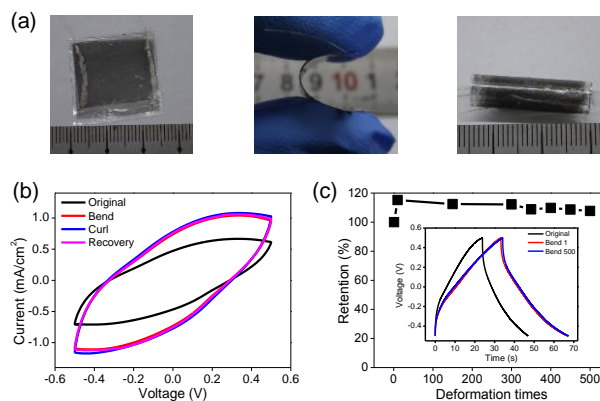


Fig. 4 (a) Photographs of deformation tests. (b) CV curves of the supercapacitors at different deformation states (60 mV/s). (c) Stability and galvanostatic charge/discharge curves of supercapacitors after 500-time bending (0.1 mA/cm^2).

In order to evaluate the flexibility of the devices, we further conducted bending and curling tests. **Figure 4a** shows the bending and curl states, the flexible device could be bent and curled to a tube. The changes of electrochemical properties during the deformation process are shown in **Figure 4b,c**. Notably, as demonstrated in the CV curves (**Figure 4b**), the area of the CV curve has been augmented by bending and curling. As a result, the areal capacitance of the device after bending was improved to 112%, and after curling was improved to 118% thanks to the favorable van der Waals forces between films and substrates and the stability of the composite electrodes produced from *in-situ* electropolymerization. The areal capacitance could maintain constant when the shape of the device was recovered to its original flat state. As shown in **Figure 4c**, the GWF+PANI device could be deformed for more than 500 times, still maintaining the areal

capacitance. At a constant current (0.1 mA/cm^2), the charge/discharge behavior of after-500-time-bending was the same to that of after-1-time-bending, and both of them was longer than before-deformation. This could be explained by the enhanced contact between electrode materials and polymer gel electrolyte during deformation process, like external pressure applied to the devices. The verified experiment has been conducted in our previous study³⁷.

Practical applications often need many supercapacitors in series in order to meet higher voltages. Therefore, we further assembled three supercapacitors in series, as shown in **Figure 5**. At the same constant current density, the voltage was extended from 1 V of single device to 3 V in series, while the current remained unchanged. After charging at 3 V, an light-emitting diode (LED) could be lighted.

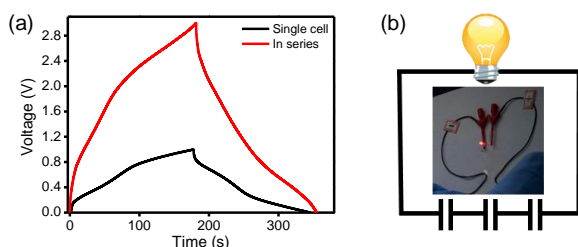


Fig. 5 (a) Galvanostatic charge/discharge curves for a single device and assembled one in series that can light (b) a LED.

Conclusion

In conclusion, a flexible, all-solid-state supercapacitor based on GWF film and polyaniline composite electrode materials was designed and fabricated at a whole thickness of is $< 1 \text{ mm}$. The synthesis and fabrication process was simple and environmental friendly. The electropolymerization of PANI has improved the areal specific capacitance from 2 to 23 mF/cm^2 with good stability after 2000 cycles. Besides the excellent flexibility, the deformation process didn't decrease the electrochemical properties but improving the capacitance to 118% of its original value. After 500 times bending, the specific capacitance and the charge/discharge behavior maintained stable. Our results suggested that the use of this graphene-based thin film electrode may lead to a new line of portable and wearable nanodevices.

Materials and Methods

Preparation of GWF: A copper mesh (150 mesh) was cleaned in hydrochloric acid and water (1:10). After nitrogen drying, the copper mesh was placed in the middle of a quartz tube located in a CVD thermal furnace. GWFs was synthesized at 1000°C with an $\text{Ar}/\text{H}_2/\text{CH}_4$ (2000/50/20 mL/min) flow. After a 15 min reaction, the sample was cooled to room temperature under argon flow. Then the cooper was etched away using a FeCl_3/HCl solution.

Electropolymerization of GWF+PANI: The mixture of polyaniline (0.5 M) and hydrochloric acid (1 M) was stirred for 1h. GWF with silver wire was used as the working electrode, Ag/AgCl as the reference electrode and Pt as the counter electrode. The electropolymerization process was controlled with potential window of 0-0.8 V in the mixture solution for several minutes.

Supercapacitors fabrication: The gel electrolyte was prepared by dissolving PVA powder (1 g) in deionized water (10 mL), heating to 90°C under stirring for 6h to form a transparent gel. After the transparent gel cool down to room temperature, H_3PO_4 (0.4 M) was blended into the mixture and stirred for 2 h. The prepared gel electrolyte was located in the hood for 72 h, to solidify. Finally, two electrodes consisting of GWFs or GWF+PANI on PETs were assembled with silver wires to fabricate supercapacitors.

Electrochemical test: The electropolymerization process was done in a three electrode system and the electrochemical test was conducted in a two-electrode system with CHI 660B electrochemical workstation (Shanghai CH Instrument Company, China).

Acknowledgements

This work was supported by National Program on Key Basic Research Project (2014CB932401) and National Science Foundation of China (51372133).

Notes and references

^aSchool of Materials Science and Engineering, State Key Laboratory of New Ceramics and Fine Processing, Key Laboratory of Materials Processing Technology (MOE), Tsinghua University, Beijing 100084, China. Email: hongweizhu@tsinghua.edu.cn

^bCenter for Nano and Micro Mechanics (CNMM), Tsinghua University, Beijing 100084, China

^cNational Center for Nanoscience and Technology, Zhongguancun, Beijing 100190, China

^dGraduate School at Shenzhen, Tsinghua University, Shenzhen 518055, China

Electronic Supplementary Information (ESI) available: SEM image, Raman spectrum and electrochemical characterizations. See DOI: 10.1039/c000000x/

- 1 J. R. Miller and P. Simon, *Science Magazine*, 2008, **321**, 651.
- 2 Y. Xu, Z. Lin, X. Huang, Y. Wang, Y. Huang and X. Duan, *Adv. Mater.*, 2013, **25**, 5779.
- 3 P. Simon and Y. Gogotsi, *Nat. Mater.*, 2008, **7**, 845.
- 4 K. S. Novoselov, A. K. Geim, S. V. Morozov, D. Jiang, Y. Zhang, S. V. Dubonos, I. V. Grigorieva and A. A. Firsov, *Science*, 2004, **306**, 666.
- 5 S. Stankovich, D. A. Dikin, G. H. Dommett, K. M. Kohlhaas, E. J. Zimney, E. A. Stach, R. D. Piner, S. T. Nguyen and R. S. Ruoff, *Nature*, 2006, **442**, 282.
- 6 A. K. Geim and K. S. Novoselov, *Nat. Mater.*, 2007, **6**, 183.
- 7 E. Frackowiak and F. Beguin, *Carbon*, 2001, **39**, 937.
- 8 Y. Shim, Y. Jung and H. J. Kim, *J. Phys. Chem. C*, 2011, **115**, 23574.
- 9 M. Winter and R. J. Brodd, *Chem. Rev.*, 2004, **104**, 4245.
- 10 T. Chen and L. Dai, *J. Mater. Chem.*, 2014, **2**, 10756.
- 11 A. Yuan and Q. Zhang, *Electrochem. Commun.*, 2006, **8**, 1173.
- 12 Z. Fan, J. Yan, T. Wei, L. Zhi, G. Ning, T. Li and F. Wei, *Adv. Funct. Mater.*, 2011, **21**, 2366.
- 13 S. Prabaharan, R. Vimala and Z. Zainal, *J. Power Sources*, 2006, **161**, 730.
- 14 Y. Lei, C. Fournier, J. Pascal and F. Favier, *Micropor. Mesopor. Mat.*, 2008, **110**, 167.
- 15 E. Frackowiak, K. Metenier, V. Bertagna and F. Beguin, *Appl. Phys. Lett.*, 2000, **77**, 2421.

- 16 C. Y. Liu, A. J. Bard, F. Wudl, I. Weitz and J. R. Heath, *Ecs. Solid State Letters*, 1999, **2**, 577.
- 17 C. Liu, Z. Yu, D. Neff, A. Zhamu and B. Z. Jang, *Nano Lett.*, 2010, **10**, 4863.
- 18 Y. Zhu, S. Murali, M. D. Stoller, K. J. Ganesh, W. Cai, P. J. Ferreira, A. Pirkle, R. M. Wallace, K. A. Cychosz and M. Thommes, *Science*, 2011, **332**, 1537.
- 19 K.H. An, W. S. Kim, Y. S. Park, Y. C. Choi, S. M. Lee, D. C. Chung, D. J. Bae, S. C. Lim and Y. H. Lee, *Adv. Mater.*, 2001,**13**,497.
- 20 L. Dai, D. W. Chang, J. B. Baek and W. Lu, *Small*, 2012, **8**, 1130.
- 21 F. Meng and Y. Ding, *Adv. Mater.*, 2011, **23**, 4098.
- 22 K. Chi, Z. Zhang, J. Xi, Y. Huang, F. Xiao, S. Wang, Y. Liu and C. Ge, *ACS Appl. mater. Inter.*, 2014,**6**,16312.
- 23 Q. Hao, W. Lei, X. Xia, Z. Yan, X. Yang, L. Lu and X. Wang, *Electrochim. Acta.*, 2010, **55**, 632.
- 24 S. Mitra, K. S. Lokesh and S. Sampath, *J. Power Sources*, 2008, **185**, 1544.
- 25 K. Zhang, L. L. Zhang, X. S. Zhao and J. Wu, *Chem. Mater.*, 2010, **22**, 1392.
- 26 Z. Xu and C. Gao, *Macromolecules*, 2010, **43**, 6716.
- 27 W. He, W. Zhang, Y. Li and X. Jing, *Synthetic Met.*, 2012, **162**, 1107.
- 28 Q. Wu, Y. Xu, Z. Yao, A. Liu and G. Shi, *Acs Nano*, 2010, **4**, 1963.
- 29 L. Wang, X. Lu, S. Lei and Y. Song, *J. Mater. Chem. A*, 2014, **2**, 4491.
- 30 X. Li, P. Sun, L. Fan, M. Zhu, K. Wang, M. Zhong, J. Wei, D. Wu, Y. Cheng and H. Zhu, *Sci. Rep.*, 2012, **2**, 395.
- 31 X. Li, X. Zang, Z. Li, X. Li, P. Li, P. Sun, X. Lee, R. Zhang, Z. Huang, K. Wang, D. Wu, F. Kang and H. Zhu, *Adv. Funct. Mater.*, 2013, **23**, 4862.
- 32 Q. Chen, X. Li, X. Zang, Y. Cao, Y. He, P. Li, K. Wang, J. Wei, D. Wu and H. Zhu, *RSC Adv.*, 2014, **4**, 36253.
- 33 R. Mažeikienė, A. Statino, Z. Kuodis, G. Niaura and A. Malinauskas, *Electrochem. Commun.*, 2006, **8**, 1082.
- 34 C. Vallés, P. Jiménez, E. Muñoz, A. M. Benito and W. K. Maser, *J. Phys. Chem. C*, 2011, **115**, 10468.
- 35 T. Lee, T. Yun, B. Park, B. Sharma, H. Song and B. Kim, *J. Mater. Chem.*, 2012, **22**, 21092.
- 36 H. Wang, Q. Hao, X. Yang, L. Lu and X. Wang, *Nanoscale*, 2010, **2**, 2164.
- 37 X. Zang, Q. Chen, P. Li, Y. He, X. Li, M. Zhu, X. Li, K. Wang, M. Zhong, D. Wu and H. Zhu, *Small*, 2014,**12**,6366.
- 38 H. Cong, X. Ren, P. Wang and S. Yu, *Energ. Environ. Sci.*, 2013, **6**, 1185.
- 39 X. Li, T. Zhao, Q. Chen, P. Li, K. Wang, M. Zhong, J. Wei, D. Wu, B. Wei and H. Zhu, *Phys. Chem. Chem. Phys.*, 2013, **15**, 17752.
- 40 W. Liu, Y. Feng, X. Yan, J. Chen and Q. Xue, *Adv. Mater.*, 2013,**23**,4111.
- 41 X. Zang, P. Li, Q. Chen, K. Wang, J. Wei, D. Wu and H. Zhu, *J. Appl. Phys.*, 2014, **115**, 024305.